Nabeel A. Abdul-Ridha, Afraah D. Salmaan, Rita Sabah, Bahjat Saeed and Najim A. Al-Masoudi*

Synthesis, cytotoxicity and *in silico* study of some novel benzocoumarin-chalcone-bearing aryl ester derivatives and benzocoumarin-derived arylamide analogs

https://doi.org/10.1515/znb-2020-0204
Received December 19, 2020; accepted March 1, 2021; published online April 3, 2021

Abstract: The development of new prostate cancer protein receptor cytochrome P450 17A1 inhibitors offers the possibility of generating structures of increased potency. To this end, the chalcone analogs **7** and **8** were prepared from treatment of methyl 3-oxo-3*H*-benzocoumarin-2-carboxylate (**4**) with aryl aldehydes. Treatment of **7** and **8** with three anti-inflammatory drugs, flurbiprofen, ketoprofen and ibuprofen, in the presence of $POCl_3$/DMAP gave the ester analogs **9**–**12**. Analogously, treatment of ethyl 3-oxo-3*H*-benzocoumarin-2-carboxylate (**15**), prepared previously from 2-hydroxy-1-naphthaldehyde (**13**) and dimethylmalonate (**14**), with various arylamines: 4-bromoaniline, 2-amino-6-methylpyridine, amino-antipyrine and 2-amino-5-nitrothiazole, in the presence of potassium *tert*-butoxide gave the benzocoumarine-3-arylamide analogs. The *in vitro* cytotoxic activities of **9**–**12** and **16**–**19** were evaluated against human prostate cancer cell lines (PC-3) and normal human liver epithelia (WRL-68) by MTT assay. Compounds **10** and **17** were the most active cytotoxic agents among the series against PC-3 cells with IC_{50} values of 71.35 and 78.25 μg mL^{-1} with SI values of 3.0 and 4.2, respectively (calculated from the cytotoxicity effects of **10** and **17** on the normal human liver epithelia [WRL-68]). Furthermore, compounds **11** and **12** were tested against breast cancer (HER2 cell lines), prostate cancer (DU-135 cell lines) and MCF-7 but were inactive. Molecular docking studies between the protein receptor CYPP450 17A1 and compounds **10** and **17** revealed that these compounds primarily form hydrophobic interactions with the receptor.

Keywords: amide analogs; benzocoumarin; breast cancer; cytotoxicity; ester derivatives; molecular docking study.

1 Introduction

Benzocoumarin compounds target a variety of biological processes and therefore are potential candidates for the treatment of a large group of diseases. Benzocoumarins have been reported to exhibit several biological activities including anti-dyslipidemia and lipid [1–3], antioxidant ([3–5], anti-inflammatory [6], antibacterial [7–9], antithrombotic [10], antituberculosis [11], antitumor [5, 12, 13] agents as well as selective inhibitors of alkaline phosphatase [14]. Some benzocoumarin analogs exhibited potential antiviral activity such bis-benzocoumarin-thiadiazine analog (**1**; Figure 1) and was found to block the function of viral neuraminidases of the influenza virus, by preventing its reproduction by budding from the host cell [15]. Meanwhile methylimidazole-methylimidazole-benzocoumarin (**2**; Figure 1) [16] exhibited promising anti-HCV activity with EC_{50} values of 5.5 μm. Further, several benzocoumarin derivatives exhibited significant antitumor activity e.g. *E*-4-(3,4-dimethoxystyryl)-2*H*-benzo[*h*]chromene-2-one (**3**; Figure 1) [17], which showed maximum antiproliferative activity in breast cancer cell lines (MDA-MB-231 and 4T1) and decreased the tumor size in the *in-vivo* 4T1 cell-induced orthotopic syngeneic mouse breast cancer model. Alternariol (3,7,9-1-methyl-6*H*-benzo[*c*]chromen-6-one) is reported to inhibit cholinesterase enzymes [18], meanwhile, it is reported to be a full androgen agonist in an *in vitro* assay [19]. In addition, it exhibited antifungal and phytotoxic activity [20]. 3,4-Benzocoumarin, a AOH (alternariol)-like compound, has the sensibility of the antibody with an IC_{50} of 919.2 ng mL^{-1} [21].

Fluorescence Imaging (FI) is one of the most popular imaging modes in biomedical sciences for the visualization

***Corresponding author: Najim A. Al-Masoudi**, Department of Chemistry, College of Science, University of Basrah, Basrah, Iraq; and Am Tannenhof 8, 78464 Konstanz, Germany, E-mail: najim.al-masoudi@gmx.de
Nabeel A. Abdul-Ridha, Department of Chemistry, College of Science, University of Qadisiya, Diwaniyaa, Iraq
Afraah D. Salmaan, Department of Chemistry, College of Education, University of Qadisiya, Diwaniyaa, Iraq
Rita Sabah, Department of Pharmaceutical Chemistry, College of Pharmacy, University of Basrah, Basrah, Iraq
Bahjat Saeed, Department of Chemistry, College of Education for Pure Science, University of Basrah, Basrah, Iraq

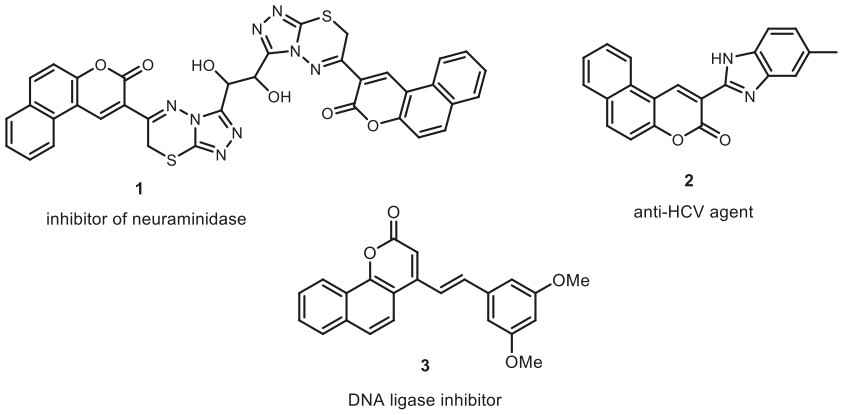

Figure 1: Some potentially active benzocoumarin analogs.

of cells and tissues both *in vitro* and *in vivo* [22]. Benzocoumarin analogs are considered as highly fluorescent imaging agents with high emission yield, excellent photostability and extended spectral range [23]. As well, they constitute the largest class of laser dyes in the blue-green region. These types of dyes have been employed as labels for fluorescent energy transfer experiments. Murata et al. [24] reported the syntheses and fluorescence properties of benzocoumarin derivatives as novel fluorophores emitting in the longer wavelength region and their application to analytical reagents, while Rajisha et al. [25] have synthesized new benzocoumarinoxadiazolyls as strong blue-green fluorescent brighteners with good bathochromic shifts.

Chalcones derivatives possess various biological, pharmacological and biocidal properties [26]. Various substitutions on both aryl rings (A and B) of the chalcones, depending upon their positions in the aryl rings, appear to influence anticancer activity by interfering with various biological targets [27, 28], meanwhile chalcone molecules with a trimethoxyphenyl unit has been reported to be the most cytotoxic (IC_{50} = 0.21 nM) derivatives synthesized so far [29].

Considering the biological significance of benzocoumarin and chalcone derivatives, herein we report the synthesis of new substituted chalcone-derived benzocoumarin scaffold, as well as their cytotoxicity on prostate cancer (PC-3 and DU-135 cells), breast cancer (MCF and HER2 cells) and an in silico molecular docking study.

2 Results and discussion

2.1 Chemistry

In the present investigation we report the syntheses of some new benzocoumarin derivatives having antitumor activity. 2-Acetyl-benzocoumarin precursor (**4**) was prepared *via* Knoevenagel reaction in basic conditions following Murthi and Basak [30] method by treatment of 2-hydroxy naphthaldeyde with ethyl acetoacetate. Treatment of **4** with 4-hydroxy- (**5**) and 4-hydroxy-3-methoxybenzaldehyde (**6**) in the presence of piperidine afforded after chromatographic purification the desired chalcone analogs **7** and **8** in 86 and 79% yield, respectively.

Next, a mild and efficient method is developed for the synthesis of esters following Chen et al. [31] method by conversion of carboxylic acids into esters through carboxyl activation by the reagent combination of $POCl_3$ and DMAP. Thus, reaction of **8** with the anti-inflammatory drugs, flurbiprofen, ketoprofen and ibuprofen, in the presence of $POCl_3$ and catalytic amount of DMAP as a base to furnish after chromatographic purification the desired esters **9**–**11** in 80, 75 and 78% yield, respectively. Similarly, treatment of **7** with ibuprofen under the same condition afforded the ester **12** in 80% yield, respectively (Scheme 1).

The structures of **7**–**12** were confirmed by their IR, ^{1}H and ^{13}C NMR and mass spectra. The benzocoumarin protons showed a similar pattern. In the ^{1}H NMR spectra of **7**–**12**, H-4 appeared as a singlet in the range δ = 8.74–8.59 ppm, while H-5 of **7**–**10** resonated as doublet (J = 7.5 Hz) or broad singlet in the range δ = 8.50–8.40 ppm. H-5 of compounds **11** and **12** overlapped with H-8 at δ = 8.39 ppm, while H-6–H-10 of compounds **7**–**12** resonated as multiplet in the range δ = 7.80–7.13 ppm. The olefinic protons H-12 and H-13 of **7** and **8** appeared in the range δ = 6.88–6.67 ppm (multiplet) and δ = 7.85–7.71 ppm (doublet, $J_{12,\ 13}$ = 16.0 Hz), respectively, whereas these protons were overlapped with other aromatic protons of compounds **9**–**12**. The aliphatic protons were fully analyzed (*c.f.* Section 4). In the ^{13}C NMR spectra of **7**–**12**, the carbonyl carbon atoms of benzocoumarin backbone C2=O and C11=O resonated in the ranges δ = 162.1–159.0 and 192.1–190.0 ppm, respectively, while the resonances in the range δ = 175.8–175.3 ppm assigned to the carbonyl carbon

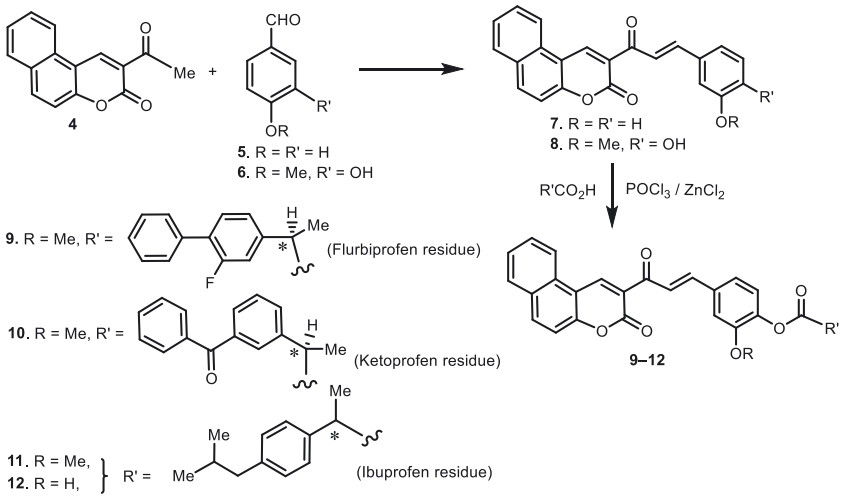

Scheme 1: Synthesis of new benzocoumarin-chalcone-derived substituted ester derivatives.

atoms C15=O of compounds **9**–**12**. Compound **10** showed signals at δ = 197.4 ppm was attributed to the carbonyl carbon atom C17=O. The resonances at the ranges δ = 138.7–132.8, 150.8–144.5 and 117.9–115.8 ppm were assigned to C-3, C-4 and C-4a, respectively. Carbon atoms C-5+C-9, C-5a and C-6 were resonated in the ranges δ = 123.1–122.7, 131.8–128.1 and 123.0–117.9 ppm, respectively. In addition, the resonances at δ = 117.4–124.6 ppm were assigned to C-10. The olefinic carbon atoms C-12 and C-13 appeared in the ranges δ = 126.2–124.6 and 145.3 and 140.5 ppm, respectively. Carbon atom C–F of compound **10** was appeared as a doublet at δ = 158.1 ($J_{C,\,F}$ = 270 Hz). The other aromatic and aliphatic substituents carbon atoms were fully analyzed (*c.f.* Section 4).

We have selected ethyl 3-oxo-3*H*-benzocoumarin-2-carboxylate (**15**), prepared previously from 2-hydroxy-1-naphthaldehyde (**13**) and dimethyl malonate (**14**) (Vahini et al. 2010) [32], as precursor for the synthesis of benzocoumarin-derived amide derivatives aiming to examine their cytotoxicity against prostate cancer. Thus, treatment of **15** with the arylamines 4-bromoaniline, 2-amino-6-methylpyridine, amino-antipyrine and 2-amino-5-nitrothiazole, in the presence of potassium *tert*-butoxide at room temperature for 30–60 min, following the method of Kim et al. [33], afforded after purification the desired amide analogs **16**–**19** in 80, 74, 60 and 65% yield, respectively (Scheme 2).

The structures of **16**–**19** were identified by ^{1}H and ^{13}C and mass spectral data, which showed similar patterns of protons and carbon atoms as those of the benzocoumarin precursor. In the ^{1}H NMR spectra, H-4 of the benzocoumarin scaffold resonated as a singlet in the range δ = 8.92–8.72, while H-5 of **16**–**18** appeared as a broad singlet at δ = 8.78, 7.98 and 7.89 ppm, respectively. H-5 of compound **19** appeared as a doublet at δ = 7.91 ppm ($J_{5,\,6}$ = 7.5 Hz), whereas H-8 of **16**–**18** resonated as a broad singlet at δ = 8.65, 7.83 and 7.68 ppm, respectively. However, the doublet at δ = 7.69 ppm ($J_{7,\,8}$ = 7.5) was attributed to H-8 of **19**. In the ^{13}C NMR spectra of **16**–**19**, the resonances at the regions δ = 158.0–157.0 and 163.6–163.0 ppm were assigned for the carbonyl carbon atoms (C-2 and C-11), respectively, whereas the carbonyl carbon atom (C-3) of pyrazole moiety (compound **18**) appeared at δ = 62.2 ppm. Atoms C-3–C4a resonated in the regions δ = 135.4–130.0, 146.0–135.1 and 118.0–116.6 ppm, respectively, while the resonances in the regions δ = 125.1–120.1, 131.8–130.8, 127.3–124.1 and 125.1–120.1 ppm were assigned to the carbon atoms (C-5–C-7), respectively. However, C-8–C-10a were appeared at the regions δ = 129.1–125.1, 131.8–130.9, 116.6–114.7 and 149.4 ppm, respectively. The resonances at δ = 61.4, 144.0 and 135.1 ppm were attributed to the carbon atoms (C-2, C-4 and C-5) of the thiazole moiety of **19**. The other aromatic aliphatic carbon atoms have been identified (*c.f.* Section 4).

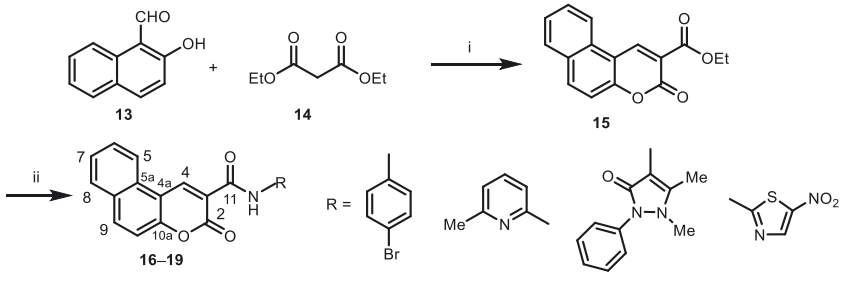

Scheme 2: Synthesis of new benzocoumarin-derived substituted arylamide derivatives. Reagents and conditions: (i) dimethyl malonate, EtOH-piperidine, reflux, 3 h; (ii) arylamines, THF, potassium *tert*-butoxide, r.t., 30–60 min.

2.2 Cytotoxic activity *in vitro*

The anticancer activities of the new benzocoumarin-chalcone-derived anti-inflammatory drugs **9**–**12** and **16**–**19** were determined *in vitro* by MTT assay [34] on cancer cell lines, human prostate carcinoma (PC-3 cell lines) and normal human liver epithelia (WRL-68), where doxorubicin was used as a positive control. The results are summarized in Table 1, and the cytotoxic effect expressed as IC_{50} values in μg mL^{-1}. After 72 h, all the complexes showed no or relatively low cytotoxicity (Figures S1 and S2, Supplementary information available online). Among the tested compounds, **10** and **17** showed the strongest dose- and time-dependent and significant cytotoxicity effect in/on PC-3 cells with IC_{50} value of 71.35 and 78.25 μg mL^{-1} (Figure 2). However, the IC_{50} values for doxorubicin were found to 17.5 μg mL^{-1} against PCa cell lines (PC-3) with selective indices (SI) of 12 and 18, respectively.

The selective index (SI) is defined as the ratio of the cytotoxicity of the tested compound with respect to normal cells (IC_{50} WRL68) versus cancer cell and used to determine the criterion of effectiveness of the compound. The SI values higher than 1.0 indicate the compounds of considerable anticancer specificity, and SI much greater than 1.0 highly selective ones. Therefore, we can conclude that **10** and **17**, of the benzocoumarin-chalcone bearing ketoprofen and 6-methyl pyridine scaffolds are excellent selective inhibitors against PCa (PC-3 cell lines) with SI = 3.0 and 4.2, respectively.

In addition, compounds **10** and **12** have been selected for further screening with other cell lines. Compound **10** was tested against breast cancer (HER2 cell lines) and prostate cancer (DU-135 cell lines) with IC_{50} values of 66.39 and 119.8 μg mL^{-1}, respectively. The cytotoxicity effects of compounds **10** and **12** were further evaluated for their toxicity against normal human liver epithelia (WRL-68) with IC_{50} = 158.4 and 254.2 μg mL^{-1}, resulting in SI values of 2.4 and 2.1, respectively (SI of doxorubicin = 9 and 14.5, respectively). Compound **12** was tested against breast cancer (MCF-7 cell lines) and noncancer cells WRL68 with IC_{50} values of 146.8 and 157.4 μg mL^{-1}, respectively, resulting of SI = 1.1 (SI of doxorubicin = 9) (Figures S3, Supplementary information). Therefore, compounds **10** and **12** showed no activity against both breast cancer (MCF-7 and HER2) and prostate cancer (DU-135).

2.3 Computational modeling study

The prostate cancer protein receptor cytochrome P450 17A1 (P450c17) has been exploited as one of the therapeutic target for PCa. In our search for new lead analogs as human CYP450 17A1 inhibitor, we have selected compounds **10** and **17** for molecular docking study. Thus, molecular docking of these two analogs into the three-dimensional P450c17 receptor structure (PDB ID: 3RUK) was performed using the Autodock program [35]. The prospective ligands were ranked according to the highest energy of the best conforms. Thus, the calculated energy scores for compounds **10** and **17** are −6.98 and −9.85, respectively, indicating selectivity and potency profiles of these analogs to bind strongly the cytochrome P450 receptor. Figure 3(A)

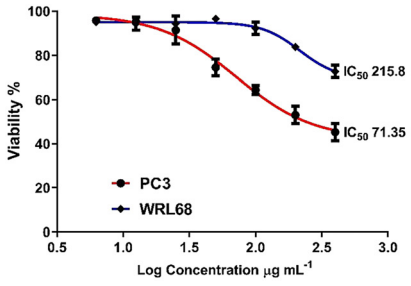

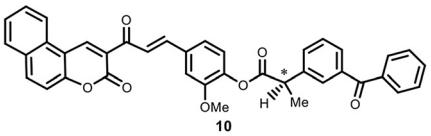

10

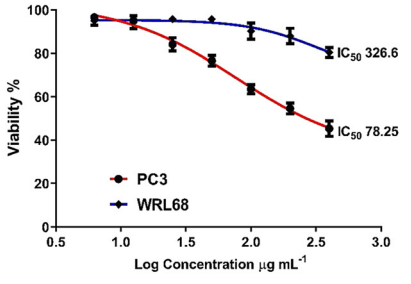

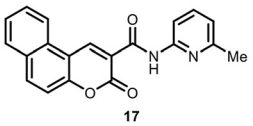

17

Figure 2: Effect of concentration of compound **10** and **17** on PC-3 and normal human liver epithelia WRL-68 cells (n = 3) for 72 h. Cell viability was evaluated by the MTT colorimeter assay.

Table 1: *In vitro* cytotoxic effects[a] of some new benzocoumarin analogs given as IC_{50}[b] in μg mL^{-1}.

Compd.	Cell line		
	PC-3	WRL68	SI
9	95.02	139.9	1.5
10	71.35	215.8	3.0
11	79.01	158.4	2.0
12	115.7	180.6	1.6
16	76.27	160.7	2.1
17	78.25	326.6	4.2
18	175.2	242.8	1.4
19	136.3	168.8	1.24
Doxo	17.5		

[a]Cytotoxic effects were expressed as IC_{50} for each cell line, obtained by MTT assay after 72 h of treatment. [b]Data represent the mean values of three independent determinations. Doxo, Doxorubicin.

demonstrated a π-π stacking interaction between the aromatic ring (f) of compound **10** and the pyrrole ring of HEM600. Additionally, it showed the same stacking between the aromatic ring (e) and Asp298. Further, aliphatic hydrophobic interactions with CYP450 17A1 receptors-binding residues including Val482, Met369, Leu370 and Val483 were observed.

According to the cytochrome CYP450 receptor docking results, Figure 3(B) demonstrated that compound **17** was able to show three π -H interactions, one between the aromatic ring (a) and Ala302, while the other interaction was observed between the pyridine residue and Ala302. The third π–H interaction was displayed between the aromatic ring (c) and Ile205. Moreover, compound **17** showed three C–H interactions of Me group of the pyridine ring with Ala367, Val366 and Val483. In addition, a π -π interaction

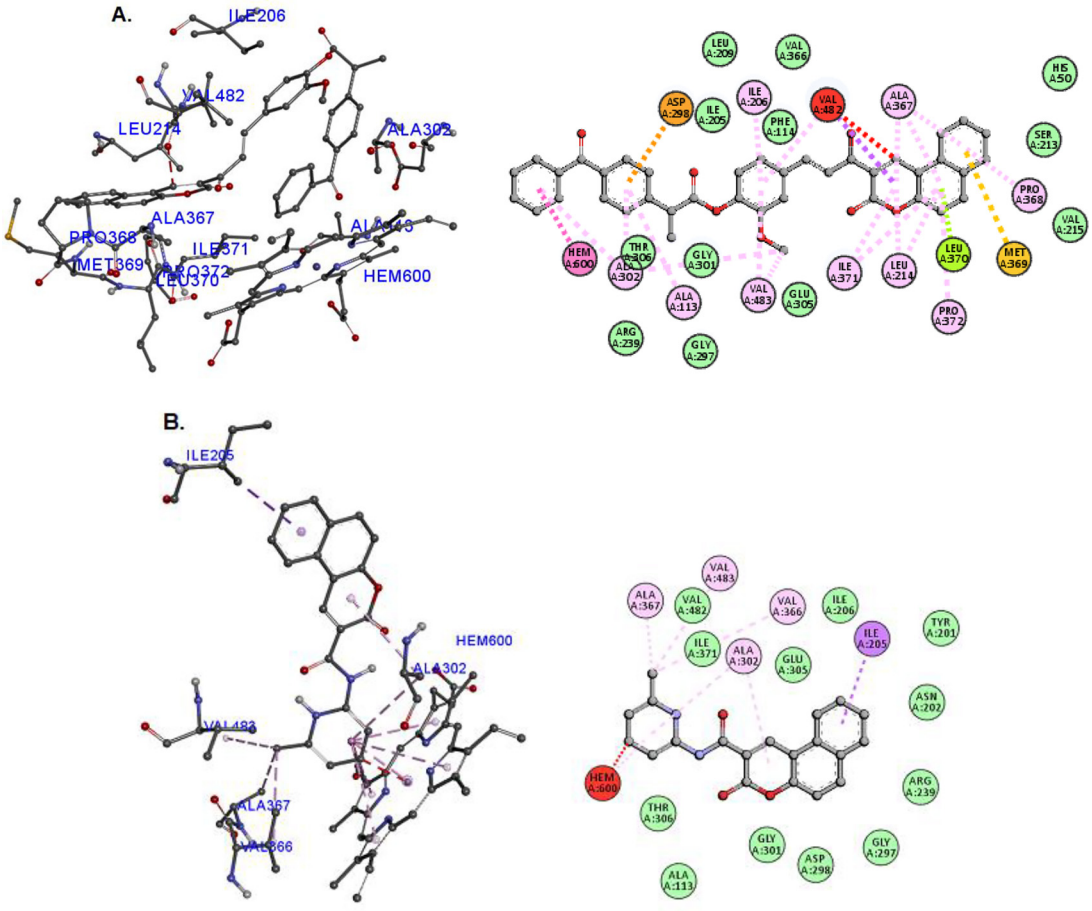

Figure 3: The interactions mode of compounds **10** (A) and **17** (B) with the active site amino acids of the human cytochrome P450 17A1 (PDB ID: 3RUK).

between pyrrole groups of HEM600 and pyridine ring was observed. Besides these interactions, nonbonding amino acids acid residues were surrounded by compounds **10** and **17** which further enhances their inhibitory activity.

3 Conclusion

In the present work, new benzocoumarin-chalcone bearing substituted ester derivatives **9**–**12** as well as benzocoumarin-derived arylamide analogs **16**–**19** have been synthesized. The structures of the new synthesized benzocoumarin analogs were confirmed by the spectral and mass data. The synthesized analogs were evaluated for their activity against prostate cancer (PC-3) and the results showed that **10** and **17** were the most active analogs of the series with IC_{50} values of 71.35 and 78.25 μg mL^{-1} (SI = 3.0 and 4.2, respectively, based on the effect of **10** and **17** on the noncancer prostate cells WRL68). Molecular docking simulations showed that analogs **10** and **17** can potentially inhibit protein receptor CYP450. Therefore, these compounds seem to be the most promising antiproliferative agents against protein receptor cytochrome P450 17A1 dependent prostatic cancer cells.

4 Experimental section

4.1 General

Melting points were determined on Stuart SMP3 melting point apparatus and are uncorrected. The IR spectra were recorded, on FT-IR Spectrophotometer (Shimaduz), using KBr discs. ^{1}H and ^{13}C NMR spectra were recorded on Varian 500 (^{1}H) and 125.65 MHz (^{13}C) spectrometers, using DMSO-*d*6 solvent containing tetramethylsilane as an internal standard (chemical shifts in δ in ppm). Mass spectra (EI, 70 eV, and FAB) were recorded on MAT 8200 spectrometers (Finnegan MAT, USA). The reactions were monitored by thin layer chromatography, (eluent: hexane-EtOAc 4: 1), and the spots were visualized by iodine and U.V.

4.2 General procedure for the synthesis of benzocoumarin-chalcone derivatives (7 and 8)

To a stirred solution of **4** (119 mg, 0.50 mmol) in EtOH (25 mL) was added arylbenzaldehyde (0.50 mmol) and aq. solution of 2 m NaOH (7 mL). After stirring at ambient temperature for 24 h, the mixture was neutralized with 1 M HCl and partitioned with EtOAc (3 × 20 mL). The combined organic extracts were washed with brine, dried over Na_2SO_4 and evaporated in vacuo. The residue was purified on a short SiO_2 column using the eluent hexane-EtOAc (3:2) as eluent to give the desired chalcone.

4.2.1 2-(3-(4-Hydroxyphenyl)acryloyl)-3*H*-benzozocoumarin-3-one (7)

From 4-hydroxybenzaldeyde **5** (61 mg). Yield: 147 mg, (86%) as orange crystals, m.p.: 270–272 °C, R_f = 0.78. – IR (KBr): ν = 3082 (Ar–H), 2939 (C–$H_{aliphatic}$), 1730 (C=$O_{lactone}$), 1680 (C=$O_{chalcone}$), 1608, 1552 (C=C) cm^{-1}. – ^{1}H NMR (DMSO-d_6): δ = 9.76 (s,1H, C–OH), 8.59 (s, 1H, H-4), 8.48 (d, 1H, $J_{5,6}$ = 7.5 Hz, H-5), 8.30 (d, 1H, $J_{7,8}$ = 7.5 Hz, H-8), 7.71 (d, 1H, $J_{12,13}$ = 15.6 Hz, H-13), 7.80 (m, 1H, H-6), 7.74 (m, 1H, H-7), 7.70–7.35 (m, 4H, H-9+H-10+H-2′+H-6′), 6.97–6.81 (m, 3H, H-12+H-3′+H-5′). – ^{13}C NMR (DMSO-d_6): δ = 190.0 (C11=O), 162.1 (C2=O) 155.8 (C–OH), 155.0 (C-10a), 147.1 (C-4), 145.3 ($C_{arom.}$-3′+C-13), 134.5 (C-3), 131.8 ($C_{arom.}$-2″+$C_{arom.}$-6″), 128.1 (C-5a+C-9), 127.8 (C-8a), 127.4 (C-8), 126.2 ($C_{arom.}$-1″+C-12), 125.7 ($C_{arom.}$-2′), 122.7 (C-5+C-6), 118.5 (C-7), 116.1 (C-4a+C-10), 115.5 ($C_{arom.}$-3′+$C_{arom.}$-5′). – MS ((+)-EI) for $C_{22}H_{14}O_4$: *m*/*z* (%) = 342 (85) $[M]^+$.

4.2.2 2-(3-(4-Hydroxy-3-methoxyphenyl)acryloyl)-3*H*-benzocoumarin-3-one (8)

From vanillin **6** (76 mg). Yield: 147 mg, (79%) as a brown crystals, m.p.: 255–256 °C, R_f = 0.73. – IR (KBr): ν = 3085 (Ar–H), 2942 (C–$H_{aliphatic}$), 1724 (C=$O_{lactone}$), 1681 (C=$O_{chalcone}$), 1610, 1572 (C=C) cm^{-1}. – ^{1}H NMR (DMSO-d_6): δ = 9.72 (s,1H, C–OH), 8.59 (s, 1H, H-4), 8.40 (d, 1H, $J_{5,6}$ = 7.4 Hz, H-5), 8.21 (br s, 1H, H-8), 7.85 (d, 1H, $J_{12,13}$ = 16.0 Hz, H-13), 7.70 (m, 1H, H-6), 7.65 (m, 1H, H-7), 7.62–7.34 (m, 3H, H-9+H-10+H-2′), 6.88 (m, 3H, H-12+H-5′+H-6′), 3.82 (s, 3H, OMe). – ^{13}C NMR (DMSO-d_6): δ = 190.4 (C11=O), 161.1 (C2=O), 154.8 (C-10a), 151.1 (C–OMe), 150.8 (C-4+C-OH), 143.5 (C-13), 132.8 (C-3), 131.2 (C-9), 129.1 (C-5a), 125.2 (C-8a+C-12), 124.3 (C-8+$C_{arom.}$-1″), 123.1 (C-12+$C_{arom.}$-6′), 122.7 (C-5+C-6), 117.9 (C-4a+C-7), 116.1 (C-10), 112.7 ($C_{arom.}$-2′), 45.4 (OMe). – MS ((+)-EI) for $C_{23}H_{16}O_5$: *m*/*z* (%) = 373 (90) $[M+H]^+$.

4.3 General procedure for the synthesis of benzocoumarin-chalcone bearing aryl ester derivatives (9–12)

To a mixture of **7** or **8** (0.60 mmol) and suitable carboxylic acid (0.5 mmol) in CH_2Cl_2 (10 mL) containing Et_3N (101 mg,

1.2 mmol) were added $POCl_3$ (77 mg, 0.5 mmol) and DMAP (19 mg, 0.15 mmol) and the mixture was stirred at room temperature for 2–3 h. After completion the reaction *via* monitoring by TLC, the mixture was evaporated to dryness and the residue was partitioned between $CHCl_3$ (3 × 10 mL) and water (10 mL). The combined organic extracts were dried (Na_2SO_4), filtered and evaporated to dryness. The residue was poured on a short column of silica gel (5 g), using hexane-EtOAc (3:2) as eluent to give the pure desired ester

4.3.1 2-Methoxy-4-(3-oxo-3-(3-oxo-3*H*-benzocoumarin-2-yl)prop-1-en-1-yl)phenyl-2-(2-fluoro-[1,1′-biphenyl]-4-yl)propanoate (9)

From **8** (171 mg) and flurbiprofen (122 mg). Yield: 239 mg, (80%) as a purple powder, m.p.: 73–75 °C, R_f = 0.49. – IR (KBr): ν = 3061 (Ar–H), 2987 (C–$H_{aliphatic}$), 1722 (C=O_{ester}), 1699 (C=Olactone), 1656 (C=$O_{chalcone}$), 1606, 1514 (C=C), 1419 (C–F) cm^{-1}. – ^{1}H NMR (DMSO-d_6): δ = 8.71 (s, 1H, H-4), 8.45 (d, 1H, $J_{5,6}$ = 7.5 Hz, H-5), 8.25 (m, 1H, H-8), 7.78 (d, 1H, $J_{12,13}$ = 16.0 Hz, H-13), 7.72–7.18 (m, 17H, Ar–H+H-12), 3.82 (s, 3H, OMe), 2.91 (br s, 1H, H-16), 1.47 (br s, 3H, Me). – ^{13}C NMR (DMSO-d_6): δ = 192.1 (C11=O), 175.3 (C15=O), 159.0 (C2=O), 158.1 (d, $J_{C,F}$ = 270 Hz, C–F), 154.3 (C-10a), 151.1 (C3′-OMe), 144.5 (C-4+C-13), 139.8 ($C_{arom.}$-4′), 135.0 (C-3+$C_{arom.}$-1″+$C_{arom.}$-1‴), 130.9 (C-5a+C-9+$C_{arom.}$-1′), 129.0, 128.5, 128.0, 127.6 ($C_{arom.}$+C-6+C-8+C-8a), 125.9 (C-12+$C_{arom.}$-5′+$C_{arom.}$-6″), 122.5 (C-5+C-7+$C_{arom.}$-6′), 116.3 (C4a + C-10+$C_{arom.}$-4″), 113.0 ($C_{arom.}$-2′), 47.1 (OMe), 44.3 (C-16), 18.8 (Me-17). – MS ((+)-EI) for $C_{39}H_{27}FO_7$: m/z (%) = 597/599 (95) $[M]^+$.

4.3.2 3-Methoxy-4-(3-oxo-3-(3-oxo-3*H*-benzocoumarin-2-yl)prop-1-en-1-yl)phenyl-2-(3-benzoyl phenyl) propanoate (10)

From **8** (171 mg) and ketoprofen (127 mg). Yield: 228 mg, (75%) as a purpule powder, m.p.: 65–66 °C, R_f = 0.57. – IR (KBr): ν = 2937 (C–$H_{aliphatic}$), 1722 (C=Oester), 1656 (C=$O_{lactone}$), 1657 (C=$O_{chalcone}$), 1600, 1512 (C=C) cm^{-1}. – ^{1}H NMR (DMSO-d_6): δ = 8.74 (s, 1H, H-4), 8.50 (br s, 1H, H-5), 8.34 (br s, 1H, H-8), 7.80–7.20 (m, 19H, Ar–H+H-12+H-13), 3.92 (br s, 3H, OMe+H-16), 1.49 (br s, 3H, Me-17). – ^{13}C NMR (DMSO-d_6): δ = 197.4 (C17=O), 191.8 (C11=O), 175.6 (C15=O), 160.5 (C2=O), 153.8 (C-10a), 150.3 (C-OMe), 147.1 (C-4), 143.4 (C-13+$C_{arom.}$-4′), 138.8 (C-3+$C_{arom.}$-1″+$C_{arom.}$-4″+$C_{arom.}$-1‴), 131.8 (C-5a+C-9+$C_{arom.}$-1′), 130.6, 130.1, 129.4, 128.4, 126.3 ($C_{arom.}$+C-6+C-8+C-8a), 125.3 (C-12+$C_{arom.}$-5′+$C_{arom.}$-6″), 122.2 (C-5+C-7+$C_{arom.}$-6′), 117.4 (C4a + C-10), 114.3 ($C_{arom.}$-2′), 47.3 (OMe), 45.1 (C-16), 18.5 (Me-17). – MS ((+)-EI) for $C_{39}H_{28}O_7$: m/z (%) = 607 (65) $[M+H]^+$.

4.3.3 2-Methoxy-4-(3-oxo-3-(3-oxo-3*H*-benzocoumarin-2-yl)prop-1-en-1-yl)phenyl-2-(4-isobutyl phenyl) propanoate (11)

From **8** (171 mg) and ibuprofen (103 mg) Yield: 218 mg, (78%) as a purple powder, m.p.: 60–62 °C, R_f = 0.50. – IR (KBr): ν = 3018 (Ar–H), 2955 (C–$H_{aliphatic}$), 1732 (C=O_{ester}), 1720 (C=$O_{lactone}$), 1656 (C=$O_{chalcone}$), 1606, 1514 (C=C) cm^{-1}. – ^{1}H NMR (DMSO-d_6): δ = 8.68 (s, 1H, H-4), 8.39 (br s, 2H, H-5+H-8), 7.85 (d, 1H, $J_{12,13}$ = 15.5 Hz, H-13), 7.75–7.13 (m, 12H, Ar–H+H-12), 3.72 (m, 4H, OMe+H-16), 2.95 (m, 2H, CH_2-18), 1.78 (m, 1H, H-19), 1.48 (br s, 3H, Me-17), 0.88 (br s, 6H, Me-20+Me-21). – ^{13}C NMR (DMSO-d_6): δ = 192.0 (C11=O), 175.8 (C15=O), 159.8 (C2=O), 152.5 (C-10a+*C3′*-OMe), 147.0 (C-4), 143.4 (C-13), 141.5 ($C_{arom.}$-4′), 138.7 (C-3+$C_{arom.}$-4″), 129.6, 128.5, 125.8 ($C_{arom.}$+C-5a + C-6+C-8+C-8a + C-9+$C_{arom.}$-1′), 124.7 (C-12), 122.9 (C-5+C-7+$C_{arom.}$-6′), 115.8 (C4a + C-10+-$C_{arom.}$-3′+$C_{arom.}$-5′), 113.7 ($C_{arom.}$-2′), 50.8 (OMe), 45.1 (C-16+C-18), 30.2 (C-19), 22.8 (Me-20+Me-21), 18.9 (Me-17). – MS ((+)-EI) for $C_{36}H_{38}O_6$: m/z (%) = 560 (75) $[M]^+$.

4.3.4 4-(3-Oxo-3-(3-oxo-3*H*-benzocoumarin-2-yl)prop-1-yl)phenyl-2-(4-isobutylphenyl) propianoate (12)

From **7** (171 mg) and ibuprofen (103 mg). Yield: 212 mg (80%) as a purpule powder, m.p.: 84–86 °C, R_f = 0.53. – IR (KBr): ν = 3061 (Ar–H), 2987 (C–$H_{aliphatic}$), 1722 (C=O_{ester}), 1699 (C=$O_{lactone}$), 1656 (C=$O_{chalcone}$), 1606, 1514 (C=C), 1419 (C–F) cm^{-1}. – ^{1}H NMR (DMSO-d_6): δ = 8.68 (s, 1H, H-4), 8.39 (br s, 2H, H-5+H-8), 7.85 (d, 1H, $J_{12,13}$ = 15.5 Hz, H-13), 7.75–7.13 (m, 12H, Ar–H+H-12), 3.72 (m, 3H, H-16), 2.95 (m, 2H, CH_2-18), 1.78 (m, 3H, H-19), 1.48 (br s, 3H, Me-17), 0.88 (br s, 3H, Me-20+Me-21). – ^{13}C NMR (DMSO-d_6): δ = 191.4 (C11=O), 175.7 (C15=O), 158.8 (C2=O), 152.9 (C-10a+C-4′), 147.6 (C-4), 140.5 (C-13), 139.5 ($C_{arom.}$-4″), 133.2 (C-3+$C_{arom.}$-1′+$C_{arom.}$-1″), 129.5, 128.6, 127.2, 126.5, 124.1, ($C_{arom.}$), 117.8 (C4a + C-10), 113.9 ($C_{arom.}$-2′), 45.0 (C-16+C-18), 30.1 (C-19), 22.7 (Me-20+Me-21), 18.9 (Me-17). – MS ((+)-EI) for $C_{35}H_{30}O_5$: m/z (%) = 531 (95) $[M+H]^+$.

4.4 Ethyl 3-oxo-3*H*-benzocoumarin-2-carboxylate (15)

This compound was prepared previously following Knoevenagel condensation reaction by refluxing 2-hydroxy-1-naphthaldehyde (**13**) (172 mg, 1.0 mmol) and dimethyl

malonate (**14**) (160 mg, 1.0 mmol) in EtOH (10 mL) in the presence of piperidine to furnish after work-up the ester **15** (227 mg, 80%). Mp and mixed melting point (114–116 °C) together with the other spectral data were identical with those of the authentic sample prepared previously [32].

4.5 General procedure for synthesis benzocoumarin-chalcone-derived substituted amide derivatives (16–19)

To a mixture of **15** (268 mg, 1.0 mmol) and arylamine (1.0 mmol) in THF (20 mL) was added potassium *tert*-butoxide (224 mg, 2.0 eq) and the mixture was stirred at room temperature for 30–60 min in the presence of air. The reaction progress was monitored by TLC. After the completion of reaction, the solution was filtered and evaporated to dryness. The residue was portioned between $CHCl_3$ (3 × 15 mL) and water (15 mL) and the combined extracts were dried (Na_2SO_4), filtered and evaporated to dryness. The residue was purified on a short column of silica gel (5 g), using hexane-EtOAc 2:1 to give the pure desired amide.

4.5.1 *N*-(4-Bromophenyl)-3-oxo-3*H*-benzocoumarin-2-carboxamide (16)

From 4-bromoaniline (172 mg). Yield: 315 mg (80%) as a greenish-white solid, m.p.: 92–94 °C, R_f = 0.44. – IR (KBr): ν = 3452 (NH_{amide}), 3063 (Ar–H), 2978 (C–$H_{aliphatic}$), 1768, 1689 (C=$O_{lactone}$+C=O_{amide}), 1610, 1562 (C=C), 1030 (C–Br) cm^{-1}. – ^{1}H NMR (DMSO-d_6): δ = 10.70 (s, 1H, NH), 8.92 (s, 1H, H-4), 8.78 (br s, 1H, H-5), 8.65 (br s, 1H, H-8), 8.29–7.69 (m, 7H, Ar–H), 7.35 (br s, 1H, H-10). – ^{13}C NMR (DMSO-d_6): δ = 163.6 (C11=O), 157.2 (C2=O), 149.0 (C-10a), 142.5 (C-4), 135.0 ($C_{arom.}$-1′), 133.4 (C-3), 130.8 (C-3+C-5a+C-9+$C_{arom.}$-3′+$C_{arom.}$-5′), 127.3 (C-6+C-8+C-8a), 125.1 (C-5+C-7), 120.9 (C-Br), 119.2 ($C_{arom.}$-2′+$C_{arom.}$-6′), 117.5 (C4a), 116.6 (C-10). – MS ((+)-FAB) for $C_{20}H_{12}BrNO_3$: m/z (%) = 416/418 (90) $[M+Na]^+$.

4.5.2 *N*-(6-Methylpyridin-2-yl)-3-oxo-3*H*-benzocoumarin-2-carboxamide (17)

From 2-amino-6-methylpyridine (108 mg). Yield: 244 mg (74%) as a colorless solid, m.p.: 87–89 °C, R_f = 0.42. – IR (KBr): ν = 3380 (NH_{amide}), 3063 (Ar–H), 2961 (C–$H_{aliphatic}$), 1743, 1699 (C=$O_{lactone}$+C=O_{amide}), 1610, 1564 (C=C), 1296 (CN) cm^{-1}. – ^{1}H NMR (DMSO-d_6): δ = 10.92 (s, 1H, NH), 8.82 (s, 1H, H-4), 7.98 (br s, 2H, H-5), 7.83 (br s, 1H, H-8), 7.25 (m, 7H, Ar–H), 6.70 (br s, 1H, $H_{pyridine}$-5′), 2.15 (Me). – ^{13}C NMR (DMSO-d_6) δ 163.2 (C11=O), 157.0 (C2=O), 155.0 ($C_{pyridine}$-2′), 151.9 ($C_{pyridine}$-6′), 148.4 (C-10a), 146.0 ($C_{pyridine}$-4′+C-4), 134.0 (C-3), 131.8 (C-9+C-5a), 125.1 (C-6+C-8), 123.2 (C-8a), 120.1 (C-5+C-7), 118.0 (C-4a), 116.6 ($C_{pyridine}$-3′), 114.7 (C-10), 112.5 ($C_{pyridine}$-5′). – MS ((+)-EI) for $C_{20}H_{14}N_2O_3$: m/z (%) = 331 (80) $[M+H]^+$.

4.5.3 *N*-(1,5-Dimethyl-3-oxo-2-phenyl-2,3-dihydro-1*H*-pyrazol-4-yl)-3-oxo-3*H*-benzocoumarin-2-carboxamide (18)

From 4-amino-1,5-dimethyl-2-phenyl-pyrazole-3-one (amino-antipyrine) (203 mg). Yield: 255 mg (60%) as a colorless solid, m.p.: 125–126 °C, R_f = 0.48. – IR (KBr): ν = 3433 (NH_{amide}), 3064 (Ar–H), 2980 (C–$H_{aliphatic}$), 1774 (C=$O_{antipyrine}$), 1763 (C=O_{amide}), 1682, 1562 (C=$O_{lactone}$), 1610, 1562 (C=C) cm^{-1}. – ^{1}H NMR (DMSO-d_6): δ = 9.68 (s, 1H, NH), 8.72 (s, 1H, H-4), 7.89 (br s,1H, H-5), 7.68 (br s, 1H, H-8), 7.48 (m, 4H, Ar–H). – ^{13}C NMR (DMSO-d_6): δ = 163.6 (C11=O), 162.2 ($C_{pyrazole}$-3′), 156.8 (C2=O), 149.0 (C-10a), 136.5 (C-4), 134.5 (C-3+$C_{arom.}$-1″), 130.9 (C-5a+C-9+$C_{arom.}$-3″+$C_{arom.}$-5″), 129.1 (C-8+C-8a), 125.1 (C-6), 123.5 (C-5+C-7), 121.8 ($C_{arom.}$-2″+$C_{arom.}$-4″+$C_{arom.}$-6″), 117.0 (C-4a), 115.3 (C-10), 103.4 ($C_{pyrazol}$-4′), 35.1 (N1′-Me), 14.9 ($C_{pyrazol}$-Me). – MS ((+)-EI) for $C_{25}H_{19}N_3O_4$: m/z (%) = 425 (78) $[M+H]^+$.

4.5.4 *N*-(5-Nitrothiazol-2-yl)-3-oxo-3*H*-benzocoumarin-2-carboxamide (19)

From 2-amino-5-nitrothiazole (145 mg). Yield: 238 mg (65%) as an orange solid, m.p.: 95–97 °C, R_f = 0.40. – IR (KBr): ν = 3456 (NH_{amide}), 3064 (Ar–H), 2980 (C–$H_{aliphatic}$), 1764 (C=O_{amide}), 1693 (C=$O_{lactone}$), 1610, 1562 (C=C), 1492 (NO_2) cm^{-1}. – ^{1}H NMR (DMSO-d_6): δ = 11.89 (s, 1H, NH), 9.46 (s, 1H, $H_{thiazole}$-4′), 8.74 (s, 1H, H-4), 7.91 (br s, 1H, H-5), 7.69 (br s, 1H, H-8), 7.48 (m, 4H, Ar–H). – ^{13}C NMR (DMSO-d_6): δ = 163.5 (C11=O), 161.4 ($C_{thiazole}$-2′), 156.7 (C2=O), 149.2 (C-10a), 144.0 ($C_{thiazole}$-4′), 135.1 (C-3+C-4+$C_{thiazole}$-NO_2), 131.8 (C-5a + C-9), 129.0 (C-8+C-8a), 124.1 (C-6), 122.0 (C-7), 120.7 (C-5), 117.1 (C-4a), 115.8 (C-10). – MS ((+)-FAB) for $C_{17}H_9N_3O_5S$: m/z (%) = 390 (90) $[M+Na]^+$.

4.6 Cytotoxicity assay

Ninety µL containing 1.0 × 104 cells of cell line suspension (PC-3, MCF-7, HER2, DU-135 and WRL68 cells) were

seeded into wells of a 96-well plate. After 24 h of incubation, 10 µL of crude extracts dissolved in 0.01% ethanol were added to final concentration 500 or 1,000 µg mL^{-1} and incubated for another 48 h. The cytotoxicity test was determined by MTT (3-(4,5-dimethylthiazol-2-yl)-2,5-diphenyltetrazolium bromide) assay [34]. In brief, 50 µL of MTT was added to the wells, the cells were cultured for additional 4 h at 37 °C. Then 100 µL of 10% SDS was added to the wells. The solubilized formazan was measured at 595 nm using microplate spectrophotometer. Each treatment was assayed in triplicate. Three independent preparations of the synthesized ligand and MTT assays were performed. Doxorubicin and 0.01% ethanol (vehicle control) were used as positive and negative controls, respectively. The cytotoxicity of the new ligands was expressed as IC_{50} value (concentration exhibited 50% cytotoxicity).

4.7 Dock and virtual screening

4.7.1 Preparations of ligands and proteins

The structures of ligands **10** and **17** were prepared by Avogadro (v. 1.0.1) [36] software and saved as PDB file formate. Then, the two ligands were prepared selecting torsions and the structures which were converted from PDB formate to PDBQT. The PDBQT files for the proteins and the ligands, united atom Kollman charges, fragmental volumes, and solvation parameters were performed by the MGLTools software. Ligand structures were energy minimized with the MMFF94 force field. The native ligands and crystallographic water molecules were removed from the PDB structures and the polar hydrogens were added before docking.

4.7.2 Grid map calculations

Autodock grid maps were calculated for each compound using AutoGrid4, based on the active site coordinates of each protein crystal structure. The size of all grid boxes $60 \times 60 \times 60$ *xyz* points with a grid spacing of 0.375 Å. The grid center dimensions were 26.18, −5.07, and 38.31 for *x*, *y* and *z*, respectively. Maps were calculated for each atom type in each ligand along with an electrostatic and desolavation map using dielectric value of −0.1465.

4.7.3 Molecular docking simulations

Molecular docking simulations were undertaken using the program Autodock [35]. Protein structures were prepared using UCSF Chimera 1.15 [37]. In Autodock program, the Lamarkian Genetic Algorithm (LGA) was used for pose sampling and the number of energy simulations was set to 2500000. The default scoring function was used for calculating the docking scores. Autogrid was used to prepare the maps. The results of molecular docking were visualized in Biovia Discovery Studio 2020 [38] and then analyzing the docking results. All docking simulations performed to validate the method, using the ligands present in crystal structures, were able to reproduce the ligand-protein interaction geometries. The image of the native ligand for 3RUK against the redocked native ligand with Autodock is shown in Figure S7 (Supplementary information), meanwhile the root-mean-square deviation of atomic positions (RMSD) was 0.405 Å.

5 Supplementary information

Cytotoxic effects of **9**, **10**, **12** and **16**–**19** on both PC-3 and WRL-68 cells (Figure S1), cytotoxic effects of **9**–**12** and **16**–**19** and doxorubicin on PC-3 cells (Figure S2), cytotoxic effects of **9** on the prostate cancer (DU-135) and breast cancer (HER2) cells as well as **12** on the breast cancer (MCF-7) cells (Figure S3) together with the image of the native ligand for 3RUK against the redocked native ligand (Figure S4) and other supporting data (^1H and ^{13}C NMR spectra of compounds **7** (Figure S5, S6), **8** (Figure S7–9), **10** (Figure S12, S13), **11** (Figure S14, S15), **12** (Figure S17), **16** (Figure S18, S19), **17** (Figure S20, S21), **18** (Figure S22, S23) and **19** (Figure S24, S25) associated with this article can be found as supplementary material in the online version (https://doi.org/10.1515/znb-2020-0204).

Acknowledgment: The authors thank the Department of Chemistry, College of Education, University of Al-Qadisiyah for providing necessary facilities.
Author contributions: All the authors have accepted responsibility for the entire content of this submitted manuscript and approved submission.
Research funding: None declared.
Conflict of interest statement: The authors declare no conflicts of interest regarding this article.

References

1. Sashidhara K. V., Kumar M., Modukuri R. K., Srivastava A., Puri A. *Bioorg. Med. Chem. Lett.* 2011, *21*, 6709–6713.
2. Sashidhara K. V., Rosaiah J. N., Kumar A., Bhatia G., Khanna A. K. *Bioorg. Med. Chem. Lett.* 2010, *20*, 3065–3069.
3. Sashidhara K. V., Rosaiah J. N., Bhatia G., Saxena J. K. *Eur. J. Med. Chem.* 2008, *43*, 2592–2596.

4. Ezzatzadeh E., Hossaini Z. *Mol. Divers.* 2020, *24*, 81–91.
5. Salem M. A. I., Marzouk M. I., El-Kazak A. M. *Molecules* 2016, *21*, 249–269.
6. Lv H.-N., Wang S., Zeng K.-W., Li J., Guo X.-Y., Ferreria D., Zjawiony J. K., Tu P.-F., Jiang Y. *J. Nat. Prod.* 2015, *78*, 279–285.
7. Gohil N. N., Kundaliya K. N., Brahmbhatt D. I. *Int. Lett. Chem. Phys. Astron.* 2016, *70*, 1–11.
8. Zaki R. M., El-Ossaily Y. A., EL-Dean A. M. K. *Russ. J. Bioorg. Chem.* 2012, *38*, 639–646.
9. Melad R., EL-Ossaily Y. A., El-Dean A. M. K. *Bioorg. Khim.* 2012, *38*, 721–728.
10. Sashidhara K. V., Kumar A., Kumar N., Sigh S., Jain M., Kikshit M. *Bioorg. Med. Chem. Lett* 2011, *21*, 7034–7040.
11. Reddy D. S., Hosamani K. M., Devarajegowda H. C. *Eur. J. Med. Chem.* 2015, *101*, 705–715.
12. Abdel-Aziem A., Rashdan H. R. M., Ahmed E. M., Shabaan S. N. *Green Chem. Lett. Rev.* 2019, *12*, 9–18.
13. El-Agrody A. M., Abd El-Mawgoud H. K., Fouda A. M., Khattab E. S. A. E. H. *Chem. Pap.* 2016, *70*, 1279–1292.
14. Channar P. A., Irum H., Mahmood A., Shabir G., Zaib S., Saeed A., Ashraf Z., Larik F. A., Lecka J., Sévigny J., Iqbal J. *Bioorg. Chem.* 2019, *91*, 103137.
15. Pavurala S., Vaarla K., Hesharwani R., Liekens S., Vedula R. R. *Synth. Commun.* 2018, *48*, 1494–1503.
16. Hassan M. Z., Osman H., Ali M. A., Ahsan M. J. *Eur. J. Med. Chem.* 2016, *123*, 236–255.
17. Hussain M. K., Singh D. K., Singh A., Asad M., Ansari M. I., Shameem M., Krishna S., Valicherla G. R., Makadia V., Meena S., Deshmukh A. L., Gayen J. R., Siddiqi M. I., Datta D., Hajela K., Banerjee D. *Sci. Rep.* 2017, *7*, 10715.
18. Osman H. M. Y., Osman M. Y. *J. High Inst. Public Health* 2008, *38*, 723–733.
19. Stypuła-Trębas S., Minta M., Radko L., Jedziniak P., Posyniak A. *Environ. Toxicol. Pharmacol.* 2017, *55*, 208–211.
20. Grover S., Lawrence C. B. *Int. J. Mol. Sci.* 2017, *18*, 18.
21. Wang J., Peng T., Zhang X., Sanlei X., Zheng P., Yao K., Ke Y., Wang Z., Jaing H. *J. Mol. Recogn.* 2019, *32*, e2776.
22. Wu Q., Merchant F. A., Castleman K. R. *Microscope Image Processing*; Academic Press: New York, 2008.
23. Al-Masoudi N. A., Al-Salihi N. J., Marich Y. A., Markus T. *J. Fluoresc.* 2015, *25*, 1847–1854.
24. Murata C., Masuda T., Kamochi Y., Todoroki K., Yoshida H., Nohta H., Yamaguchi M., Takadate A. *Chem. Pharm. Bull.* 2005, *53*, 750–758.
25. Rajesha G., Kumar H. C. K., Naik H. S. B., Mahadevan K. M. *S. Afr. J. Chem.* 2011, *64*, 88–94.
26. Albuquerque H. M. T., Santos C. M. M., Cavaleiro J. A. S., Silva A. M. S. *Curr. Org. Chem.* 2014, *18*, 2750–2775.
27. Das M., Manna K. *J. Toxicol.* 2016, *2016*, 7651047.
28. Gao F., Huang G., Xiao J. *Med. Res. Rev.* 2020, *40*, 2049–2084.
29. Lawrence N. J., Rennison D., McGown A. T., Hadfield J. A. *Bioorg. Med. Chem. Lett.* 2003, *13*, 3759–3763.
30. Murthi G. S. S., Basak M. *J. Indian Chem. Soc.* 1993, *70*, 170–171.
31. Chen H., Xu X., Liu L., Tang G., Zhao Y. *RSC Adv.* 2013, *3*, 16247–250.
32. Vahini M. V., Devarajegowda H. C., Mahadevan K. M., Meenakshid T. G., Arunkashi H. K. *Acta Crystallogr.* 2010, *E66*, o2658.
33. Kim B. O., Lee H.-G., Kang S.-B., Yoon Y.-J. *Synthesis* 2012, *44*, 42–50.
34. Mosmann T. *J. Immunol. Methods* 1993, *65*, 55–63.
35. Morris G. M., Huey R., Lindstrom W., Sanner M. F., Belew R. K., Goodsell D. S., Olson A. J. *J. Comput. Chem.* 2009, *16*, 2785–2791.
36. Hanwell M. D., Curtis D. E., Lonie D. C., Vandermeersch T., Zurek E., Hutchison G. R. *J. Cheminf.* 2012, *4*, 17.
37. Pettersen E. F., Goddard T. D., Huang C. C., Couch G. S., Greenblatt D. M., Meng E. C., Ferrin T. E. *J. Comput. Chem.* 2004, *13*, 1605–612.
38. Biovia Discovery Studio. *Discovery Studio Modeling Environment*; Dassault Systêmes: San Diego (USA), 2020.

Supplementary Material: The online version of this article offers supplementary material (https://doi.org/10.1515/znb-2020-0204).